

NUMBER AND LUMINOSITY EVOLUTION OF INTERACTING GALAXIES AS A NATURAL EXPLANATION FOR THE GALAXY COUNTS

Pedro Colín¹

Instituto de Astronomía
Universidad Nacional Autónoma de México

Received 1994 October 20; accepted 1995 May 8

RESUMEN

En el marco del modelo para el conteo de galaxias de Colín, Schramm, & Peimbert, consideramos un modelo de fusión para explicar el exceso de galaxias observado en el conteo de galaxias en la banda azul. El exceso se explica por la evolución de la luminosidad y la densidad numérica de un grupo de galaxias llamadas interactuantes, I. Suponemos que la densidad numérica de galaxias I aumenta como $(1+z)^\eta$ debido a la fusión de galaxias. Por otra parte, proponemos que su luminosidad característica aumenta como $(1+z)^3$, debido a brotes de formación estelar generados por la colisión entre galaxias y que disminuye como $(1+z)^{-\eta}$ debido al cambio en su tamaño. Un modelo con $\eta = 4.0$ predice que cerca del 17% de las galaxias a $z = 0.4$ están interactuando. Modelos de evolución en la densidad numérica con valores altos de η ajustan mejor los datos; en particular, el modelo con $\eta = 4.0$ predice que cerca del 13% de las galaxias tienen $z > 0.7$ en el intervalo $21.0 < m_{b_j} < 22.5$. Esto contrasta con el límite superior del 5% obtenido por Colless et al. (1990, 1993). El exceso de galaxias con alto corrimiento al rojo no se puede explicar simplemente cambiando los parámetros de la función de luminosidad de las galaxias I. Este resultado nos indica que la fusión de galaxias no es la historia completa.

ABSTRACT

A newly developed isochrone synthesis algorithm for the photometric evolution of galaxies is described. Two initial mass functions and three photometric transformations are used to compute the $B - V$ and $V - K$ color index evolution. Non-negligible differences are observed among different models.

In the framework of the galaxy count model by Colín, Schramm, & Peimbert a simple merging scenario is considered to account for the excess of galaxies observed in the blue band counts. The excess is explained by the number and luminosity evolution of a group of galaxies called interacting, I. It is assumed that the number of I galaxies increases as $(1+z)^\eta$ due to mergers. Moreover, it is proposed that their characteristic luminosity increases as $(1+z)^3$ due to starbursts driven by galaxy-galaxy collision and decreases as $(1+z)^{-\eta}$ due to the change in the size of the galaxies. A model with $\eta = 4.0$ predicts that about 17% of the galaxies at $z = 0.4$ are interacting. Number evolution models with a rather high value of η fit better the data; in particular, the model with $\eta = 4.0$ predicts that about 13% of the galaxies have $z > 0.7$ in the $21.0 < m_{b_j} < 22.5$ interval, this contrasts with the upper bound of 5% obtained by Colless et al. (1990, 1993). The excess of high redshift galaxies cannot be simply explained by changing reasonably the parameters of the luminosity function of I galaxies. This result could indicate that mergers are not the whole story.

Key words: **GALAXIES – LUMINOSITY FUNCTION, MASS FUNCTION**

1. INTRODUCTION

The excess number density of galaxies observed in the blue band (e.g. Tyson 1988; Metcalfe et al. 1991; Lilly, Cowie, & Gardner 1991) over the expected value from a non-evolving model has generated great interest. Several possible explanations have been suggested to account for it: from those that invoke a non-zero cosmological constant that provides a greater volume to accommodate the excess number of galaxies (Yoshii & Takahara 1988; Fukugita et al. 1990; Yoshii 1993), to those that assume evolution of the luminosity function of galaxies (LFG) via an increase in the number density of galaxies due to mergers (Guiderdoni & Rocca-Volmerange 1987; Broadhurst, Ellis, & Glazebrook 1992; Colín, Schramm, & Peimbert 1994, hereafter CSP) or via an increase in the characteristic luminosity of the LFG due to starbursts driven possibly by galaxy-galaxy collisions (Carlberg & Charlot 1992). Moreover, faint redshift surveys by Broadhurst, Ellis, & Shanks (1988) and Colless et al. (1990, 1993) place galaxies quite near; the median redshift is just ~ 0.2 and ~ 0.3 , respectively. In addition, no galaxies were found with $z > 0.7$ brighter than $b_J = 22.5$ ($b_J \simeq B - 0.3$) in the sample by Colless et al. This result imposes a strong constraint on evolving models. In these models a non-negligible fraction of galaxies with $z > 0.7$ is expected, indeed larger than the one predicted by a non-evolving model.

With the advent of infrared arrays and infrared CCD detectors it is also possible to count galaxies deeply in the K -band (Cowie et al. 1994; Soifer et al. 1994). Surprisingly, a non-evolving model fits relatively well the K -counts. This almost rules out models with non-standard cosmologies, as the ones with a non-zero cosmological constant, since in this case they overestimate the number of galaxies. Yet, the observational restrictions admit one more explanation, namely a new population of blue galaxies at $z > 0.2$ that faded or were disrupted so as to become invisible at present (Cowie, Songaila, & Hu 1991; Babul & Rees 1992).

Local low surface brightness galaxies have similar physical properties to those observed in the faint blue excess population (McGaugh 1994). McGaugh suggests that the excess is made up of low surface brightness galaxies and his idea rests on a bivariate LFG; that is, a LFG that—in addition to type—depends on surface brightness.

The result that faint blue galaxies (FBGs) are weakly clustered (Efstathiou et al. 1991) has been sometimes taken as an evidence against the merger-driven explanation for the observed excess of FBGs (see, for instance, Babul & Rees 1992; McGaugh

1994); the low value for the angular correlation function at $30''$ is explained by Efstathiou et al. assuming that most FBGs belong to a population that is weakly clustered and intrinsically faint at the present epoch. This result is challenged by a recent work by Cole et al. (1994) where no evidence is found for the evolution of the comoving correlation length with redshift to $B = 22$; however a more recent paper by Infante & Pritchet (1994) supports the earlier results by Efstathiou et al.

The hypothesis that the observed excess of FBGs is due to an increase in the number density of galaxies that are strongly interacting, the merger-driven excess, is retaken here. A phenomenological model was developed in CSP to account for three different observational restrictions, namely: (1) the B -counts, (2) the K -counts, and (3) a B -redshift distribution. It was due to the increase in the number density of a type of galaxies, called interacting (I), that the observations were fitted.

This kind of model—like others of similar nature—is supported by a recent work on high-resolution imaging of faint blue galaxies (Colless et al. 1994) and by *HST* studies of morphology of high redshift galaxies (Griffiths et al. 1994a, b). Colless et al. find, from a sample of 26 galaxies which belong to the redshift survey of Colless et al. (1993), 17 galaxies that have an enhanced star formation rate indicated by [O II] equivalent widths greater than 20\AA . About 30% of these galaxies have companions at projected distances closer than $10\text{ h}^{-1}\text{ kpc}$.

This model differs from the one by CSP in the following: (1) a different algorithm for the computation of the ‘passive’ luminosity evolution correction is applied, and (2) the total luminosity of the I galaxies, L_I^T , is not conserved because of the starbursts driven by galaxy-galaxy collisions. This is what we call ‘active’ luminosity evolution. The model in this paper also differs from the one by CSP in the assumed values for the parameters of the luminosity functions of the different types of galaxies; in particular, those values assumed for the characteristic luminosities of Sa-c and E/SO galaxies. Because they are fainter in CSP, they produce a better fit for the redshift distribution than the one we show in this paper.

An outline of the paper follows: in § 2 we briefly discuss our revised color evolution code with an isochrone synthesis algorithm, in § 3 our merger-driven model is described, and in § 4 we present our conclusions.

2. COLOR EVOLUTION OF GALAXIES

2.1. Model

Our photometric evolution of galaxies code is fully discussed in CSP therefore here just a brief review will be given. Unlike CSP where a standard proce-

¹ Present address: Universidad de Toronto, Dept. of Astronomy, Canada.

ture was used (e.g., Bruzual 1983) here an isochrone synthesis algorithm is implemented. The advantages of this algorithm have been discussed elsewhere (e.g., Charlot & Bruzual 1991), we just would like to mention the usefulness of the algorithm in computing color evolution properties for short ($\sim 10^8$ yr) time-scales of the star formation rate.

2.1.1. Ingredients

The ingredients necessary in any spectrophotometric evolution of galaxies code are four: (1) a library of stellar evolutionary tracks, (2) a library of stellar spectra, (3) an initial mass function (IMF), and (4) a star formation rate (SFR). Our compiled tracks are from Schaller et al. (1992) for solar metallicity. These tracks are incomplete and therefore we had to complete them. Tracks from other authors were used and various useful simplifications were made; in particular, the lifetime of the asymptotic giant branch was left as a free parameter. This will be remedied as soon as the evolutionary models for the horizontal and asymptotic giant branch from the group of Maeder and collaborators are incorporated. As long as we are only interested in galaxy color evolution there is no need for having a library of stellar spectra, we just need a photometric transformation from the HR theoretical diagram to the observational one. The compilation work by Schmidt-Kaler (1982) has been used now to pass from one diagram to the other. We still continue to use the work by Johnson (1966) to get the rest of the color indexes.

The IMF is normalized so that,

$$\int_{m_{low}}^{m_{up}} m\phi(m)dm = 1 \quad (1)$$

Although a value of $0.1 M_{\odot}$ is often used for m_{low} , as we do, we should keep in mind that the contribution by substellar objects to the integrated infrared light of a galaxy might not be negligible. Of course, this depends on the luminosity function of these objects of which we know nothing. From chemical evolution considerations Peimbert, Sarmiento, & Colín (1994) limit the amount of substellar objects in the solar neighborhood to $< 0.02 M_{\odot} \text{ pc}^{-3}$. The recent IMF determination by Kroupa, Tout, & Gilmore (1993), KTG IMF, for the solar vicinity is used, as a good guess, for the IMF for a variety of types of galaxies. Nevertheless, the "standard" Salpeter IMF, S IMF, with the exponent $x = 1.35$ is used for comparison purposes. A value of $60.0 M_{\odot}$ is taken for m_{up} .

In view of the great uncertainties about stellar formation histories of galaxies, an exponential law for the SFR is usually taken to model the color evolution of the different types of galaxies. The maximum virtue of this scheme is that almost all present galaxy colors can be reproduced by varying the time scale, τ ,

of the SFR: from an elliptical galaxy, $\tau = 0.5$, to an irregular one, $\tau = \infty$ (e.g., Charlot & Bruzual 1991; CSP). These galaxy colors are, of course, metallicity-dependent. This effect is now being incorporated in the latest models for spectral evolution of galaxies; in particular, for elliptical galaxies see Worthey (1994 and references therein). The evolutionary correction, e-correction, to the counts should not worry us too much because as we know from CSP there are only three types of galaxies that play an important role on the counts. According to our count-scheme, the luminosity of a galaxy belonging to the interacting group of galaxies does not evolve; i.e., it has no e-correction. We can be confident that the other two types, E/SO and Sa-c, are being modeled relatively well.

2.1.2. Isochrone Synthesis Algorithm

The luminosity of a single stellar population (SSP) is given by

$$l_{\Delta\lambda}(t) = \int_{m_{min}}^{m_{max}} 10^{-0.4(M_{\Delta\lambda} - M_{\Delta\lambda,\odot})} \phi(m) dm \quad (2)$$

where m_{min} is the lower limit of the IMF and m_{max} is the maximum mass in the isochrone with age t . The integrated luminosity for a composite stellar population, with a history of star formation given by $\psi(t)$, can be obtained with the convolution integral

$$L_{\Delta\lambda}(t) = \int_0^t \psi(t-t') l_{\Delta\lambda}(t') dt' \quad (3)$$

The isochrone at time t from a complete set of evolutionary tracks is built as follows: let us assume that the tracks are divided into n stages, from zero age main sequence (ZAMS) to post-asymptotic giant branch (P-AGB). The indexes i and j number the stages and the tracks, respectively, with $i = 1, \dots, n$ and $j = 1, \dots, m$. The mass of the star at the stage i is given by

$$\log m_i(t) = A_{i,j} \log(M_{j+1}) + (1 - A_{i,j}) \log(M_j) \quad (4)$$

where

$$A_{i,j} = \frac{\log t_{j,i} - \log t}{\log t_{j,i} - \log t_{j+1,i}} \quad (5)$$

In equation (5) $t_{j,i}$ denotes the age of the star of ZAMS-mass M_j at the i^{th} evolutionary stage, where

$$t_{j+1,i} \leq t < t_{j,i}$$

and

$$M_j \leq m_i(t) < M_{j+1} .$$

M_1 and M_m denote the lower and upper limit of the IMF, respectively. This procedure is performed for each stage (value of i). The HR diagram physical parameters, $\log L$ and $\log T_{eff}$, associated to the star of mass m_i are obtained by interpolating the tracks between the stars of masses M_j and M_{j+1} .

To obtain the integrated properties of this SSP we proceed as Bruzual (1992): the number of stars of mass m_i , $n(m_i)$, is found by integrating the IMF from m^- to m^+ , where $m^- = \sqrt{m_{i-1}m_i}$ and $m^+ = \sqrt{m_i m_{i+1}}$. The luminosity, $l_{\Delta\lambda,i}$, is then computed by assigning $N_{i,j} = A_{i,j}n(m_i)$ stars to the HR parameters of the star of mass M_{j+1} at the i^{th} stage, and $N_{i,j+1} = (1 - A_{i,j})n(m_i)$ to the star of mass M_j at the same i^{th} stage. We finally obtain $l_{\Delta\lambda}(t)$ by summing over all i 's.

2.2. Results

In computing photometric evolution of galaxies special care should be taken with the photometric transformation. This is stressed in Figure 1 where the $B - V$ and $V - K$ evolution is plotted for a 1-Gyr burst SFR, for three different calibrations. The dotted line uses a compilation work by Schmidt-Kaler (1982) and Johnson (1966), the solid line utilizes one from Schmidt-Kaler (1982) and Bessel & Brett (1988), and the dashed line comes from a compiled calibration work by Bruzual & Charlot (1993). The greatest difference among them amounts to ~ 0.25 mag in $V - K$ at around 1.7×10^7 yr; this difference is due to the $V - K$ values adopted for the giant luminosity class at the low-temperature regime. The peak at 1.7×10^7 yr is produced by the supergiant red branch contribution. Hereafter the calibration by Schmidt-Kaler (1982) and Bessel & Brett (1988) will be used. In Figure 2 we have plotted the $B - V$ and $V - K$ color evolution for a 1-Gyr burst SFR, in this case for two different IMFs: the KTG IMF (solid line) and the Salpeter one (dotted line). The $V - K$ color is slightly bluer when computed with the KTG IMF, the greatest difference at $\sim 10^8$ yr amounts to 0.1 mag. A much smaller difference is observed for the case of $B - V$.

3. A MERGER MODEL FOR GALAXY COUNTS

This paragraph describes briefly the $\Omega_0 = 1$ merger model for galaxy counts of CSP. Galaxies were divided into five different types: E/SO, dE/dSO (spheroidal dwarfs), Sa-c (spirals), dI (dwarf irregulars), and I (interacting galaxies). A Schechter analytical representation for the galaxy luminosity function was used for all types. It was shown that a Gaussian representation for the luminosity function

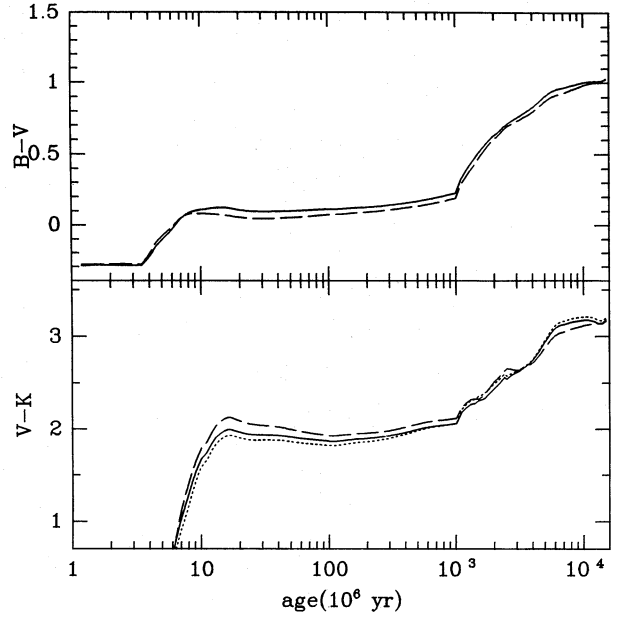


Fig. 1. Evolution of the color indices $B - V$ and $V - K$ for a 1-Gyr burst SFR with three different photometric calibrations: Bruzual & Charlot (dashed line), Schmidt-Kaler and Bessel & Brett (solid line), and Schmidt-Kaler and Johnson (dotted line).

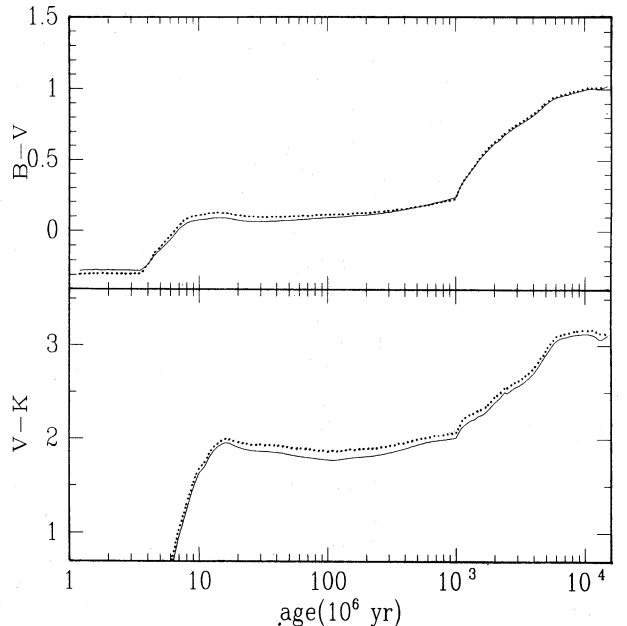


Fig. 2. As in Figure 1 we have plotted the evolution of the color indices $B - V$ and $V - K$ for a 1-Gyr burst SFR. The two curves come from two different IMFs: KTG IMF (solid line) and Salpeter IMF (dotted line). The calibration from Schmidt-Kaler and Bessel & Brett has been used.

(LF) of the brighter galaxies provided a poor fit to the redshift distribution. CSP models were based on a scenario where the amplitude of the LF of I galaxies, ϕ_I^* , increased with redshift as a power law; i.e., $\phi_I^* \propto (1+z)^\eta$. The k-corrections for the different classes of galaxies were obtained from the spectral energy distributions (SEDs) by Coleman, Wu, & Weedman (1980) and Pence (1976); in particular, the SED for an average elliptical galaxy was taken to be the SED of the bulge of M31. The e-corrections were evaluated from our standard approach to the photometric evolution of galaxies.

3.1. The Interacting Galaxies

The I group does not form properly a morphological group of galaxies, it is rather composed of pairs of strongly interacting galaxies of different nature. Moreover, the observed physical characteristics of the faint galaxies such as: their blue colors, enhanced star formation, indicated by [O II] equivalent widths greater than 20 Å (Colless et al. 1994), etc. give us information about the nature of the galaxies that intervene in the interactions. These characteristics, which are often associated to a system of interacting galaxies, seem to indicate that the type of galaxies that are participating in the mergers are gas-rich galaxies (e.g., Carlberg & Charlot 1992). This is a point worth noting since we will see below that the increase of the characteristic luminosity of the I galaxies, L_I^* —to a first approximation—is due to the starbursts driven by cloud-cloud collision. It will be assumed that the I-galaxy LF (LFI) follows a Schechter form.

The evolution of LFI is due to three factors: (1) a greater number density, (2) a larger gas content that results in a stronger starburst, and (3) a smaller average size. The points (2) and (3) go in opposite direction, whereas the point (2) increases L_I^* while the point (3) decreases it. It is interesting to note that in the absence of starbursts the effects on B -counts by points (1) and (3) cancels out. This might be the case for the K -counts where most of the light comes from a population of old stars.

Our merger model scenario for the galaxy counts is then the following: suppose that at each time a photograph of the Universe is taken and that galaxies are divided into various types. Those that show signs of strong interaction are brought to the I group of galaxies. As we look back in time we see that the number density (per comoving volume) of I galaxies increases, while, by hypothesis, the number density of the other types of galaxies does not change. The increase in the total luminosity of I galaxies ($\propto L_I^* \phi_I^*$) is due to the their greater amount of gas as well as their increasing number density.

In this paper the above scenario for the modeling of the B -, K -counts, and the redshift distribu-

tion is used and compared with observations. We propose that the L_I^* of both the B -band and the K -band evolves due to galaxy-galaxy collision and due to the change in size, yet a model for the K -counts where the contribution from starbursts is neglected is also computed. The galaxy-galaxy collision term, the one which produces an ‘active’ luminosity evolution, contributes with $(1+z)^3$ to L_I^* and it comes from assuming that: (a) L_I^* is proportional to the stellar formation, Ψ , driven by the mergers, (b) in a cloud-cloud collision $\Psi \propto \sigma^2$, where σ is the gas density, and (c) $\Omega_0 = 1$. On the other hand, L_I^* is reduced by $(1+z)^{-\eta}$ due to the change in size. Models with different values of η are calculated.

A Schechter analytical representation is used for the LFI, with relative freedom in choosing its α and M^* parameters due to the great uncertainty about its shape. Its characteristic luminosity, the luminosity at the “knee” of the LF, is assumed to be greater than the corresponding value for elliptical and spiral galaxies. The fraction of I galaxies that contributes to the LFG is assumed greater than the amount of mergers observed at the present epoch (1–2%) in order to improve our fit to the B -counts.

3.2. Ingredients

In Table 1 the values of the parameters of the luminosity functions of the different galaxy classes are shown: second, third, and fourth columns. In the fifth, sixth, an seventh columns the timescale of the SFR, the $B-V$ and $B-K$ color indices are shown, respectively. These were computed by using the photometric evolution code described in § 2. The last column indicates the kind of SED used for each type of galaxy; in particular, the SED of the bulge of M31 is used for E/SO galaxies.

The assumed values for α , M^* , and the mix reflect several facts. First, the values for the parameters α and M^* of the LF of spiral galaxies are similar to those derived by Loveday et al. (1992) for the field LFG. Second, there is still much uncertainty about the value of α for early-type galaxies, the rather steep value assumed in this paper, as compared with those obtained by several authors (Efstathiou et al. 1988; Loveday et al. 1992; Zucca, Pozzetti, & Zamorani 1994), fits better the K -counts. Third, there is not yet a field LF for early-type dwarf galaxies nor for late-type dwarfs, though we use the α and M^* values of the LF of dE/dSO galaxies and the M^* value of the LF of dI galaxies obtained by Sandage, Binggeli, & Tammann (1985) for the Virgo cluster; needless to say that there is no reason to expect that these assumptions are correct. Fourth, the parameters for the LFI are chosen in such a way that: (1) the characteristic luminosity is greater than the one for E/SO galaxies, (2) the slope at the faint end equals that of the total luminosity function, and (3) the fraction of I galaxies should be small. At the end, our mix takes

TABLE 1

INPUT PARAMETERS OF THE MODELS

Type	α	M^*	Mix	τ^a (Gyr)	$B - V^b$	$B - K^b$	SED ^c
I	-1.20	-21.2	0.05	∞	0.49	3.04	Sdm
dI	-1.40	-16.2	0.16	∞	0.49	3.04	Sdm
Sa-c	-0.80	-20.0	0.30	5.0	0.70	3.54	Scd
dE/dSO	-1.35	-18.0	0.30	5.0	0.70	3.54	Sab
E/SO	-1.00	-20.7	0.19	0.5	1.01	4.17	M31

^aThe star formation rate used to derive the color of the galaxies at the present epoch is: $\psi \propto e^{-t/\tau}$.

^bTwo local color indices representatives of the different types of galaxies, computed by our photometric evolution of galaxies code.

^cThe spectral energy distributions, SEDs, are from CWW and Pence 1976; in particular, for E/SO galaxies we have taken the SED of the bulge of M31.

into account the following facts: (1) the uncertainty in the fraction of strongly interacting systems, (2) there are more spiral galaxies than elliptical galaxies in the surveys of Efstathiou et al. and Loveday et al., (3) there is a significant fraction of dE/dSO galaxies in clusters (Ferguson & Sandage 1991), in the poorest cluster, the Leo group, about 46% are dE/dSO galaxies, and (4) recent determinations of the LFG (Eales 1993; Lonsdale & Chokshi 1993) are producing a steeper slope at the faint end (~ -1.3).

The e-corrections are evaluated assuming an exponential decreasing SFR with a varying timescale. For dwarf galaxies, spheroidal and irregulars, it appears inappropriate to model their light with a solar metallicity population. Furthermore, a choice for the SFR becomes difficult; dwarf irregular galaxies are better modeled by a series of star formation bursts followed by periods of zero star formation (e.g., Pilyugin 1993). The number and the strength of the bursts, and the duration of the quiescent periods are parameters that seem to depend on the galaxy. Fortunately, these galaxies make a negligible contribution to the B - and K -counts except for the fainter end (e.g., CSP). The I galaxies have no e-correction by hypothesis.

3.3. Results

The detection rate and selection effects, according to Yoshii (1993), were evaluated but they were not incorporated to our models. The reason is the small effect they have on the predicted B -counts. In an isophotal magnitude scheme, $S_L = 29 B$ mag arcsec⁻², with an imposed minimum diameter of $D_{min} = 2.0''$, a detection rate of about 75% at $B = 26$ is expected in a $(\Omega_0, \Lambda_0) = (1, 0)$ scenario. This amounts to a difference of just 0.10 dex at $B = 26$ (see also Yoshii).

In Figure 3 the number of galaxies vs. blue magnitude is plotted for four models. The data are from Maddox et al. (1990), Lilly et al. (1991), and Metcalfe et al. (1991). There are two non-evolving, NE, models: one with the parameter values from Table 1 (NE) and the other one (NE KGB) with the parameter values from Koo, Gronwall, & Bruzual (1993, hereafter KGB). The Table 2 from KGB was uti-

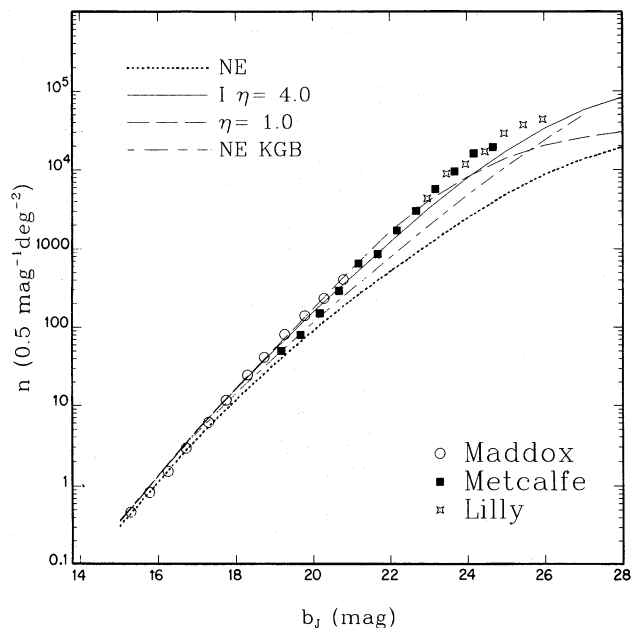


Fig. 3. The number of galaxies vs. blue magnitude is plotted for four models: two are non-evolving, NE, and the other two are merger-driven, for two values of η .

lized to derive the Schechter parameters for the I ($B - V < 0.6$), Sa-c ($0.6 \leq B - V < 0.85$), and E/SO ($B - V \geq 0.85$) classes of galaxies, these are:

$$(\alpha, M^*, \phi^*) = \begin{cases} (-1.86, -21.6, 9.93 \times 10^{-5}) & \text{for I,} \\ (-1.13, -21.8, 3.29 \times 10^{-4}) & \text{for Sa - c,} \\ (-1.38, -20.1, 9.90 \times 10^{-4}) & \text{for E/SO.} \end{cases}$$

The inclusion of the NE KGB model in Figure 3 is with the purpose of showing that a much smaller difference is obtained between a NE model and the observations if the parameters of the LFs are moved in the 'correct' direction. The other two models plotted in this figure are merger-driven models for two values of η . A significant difference is starting to observe between each other at $b_J > 25$ ($b_J \simeq B - 0.3$). Moreover, the maximum difference between the data and our $\eta = 4.0$ model amounts just 0.2 dex at $b_J = 25.0$.

When the LFG is parameterized by a Schechter function, the number density, n_0 , is related to the amplitude of the LFG, ϕ^* , by

$$n_0 = \phi^* \Gamma(1 + \alpha, \beta) ,$$

where Γ is the incomplete gamma function and β is the faint luminosity limit in units of L^* . Our LFG is a composite LF, the sum of five different Schechter LFs, therefore the parameters α , ϕ^* , and M^* are not well defined. Yet, approximate values for α , ϕ^* , and M^* can be obtained by attempting to fit our LFG to a Schechter function. When this is done, (see Figure 4) we get the following: $\alpha = -1.20$, $M^* = -20.7$, and $\phi^* = 1.66 \times 10^{-3} \text{ Mpc}^{-3}$. It is encouraging to note that the value we get for ϕ^* , necessary to fit the brighter part of the B -counts, is similar to those derived by several authors (Efsthathiou 1988; de Laparent, Geller, & Huchra 1989; Loveday et al. 1992).

In Figure 5, the number distribution in the K -band is plotted for the same models as for the B -band except that here, the NE KGB model is replaced by a merger-driven model in which the L_I^* in the K -band does not increase due to the starbursts (model denoted by II $\eta = 4.0$). The data are from a compilation by Gardner, Cowie, & Wainscoat (1993). It is important to point out here the better agreement obtained by those models with a rather high value of η . A redshift distribution is plotted in Figure 6 for two intervals of B magnitude. The histograms are redshifts for 125 galaxies taken from Broadhurst et al. (1988) in the $20.0 \leq b_J \leq 21.0$ range and for 78 galaxies taken from Colless et al. (1990, 1993) in the $21.0 \leq b_J \leq 22.5$ interval, this later survey is complete to 4.5%. Our merger-driven models predict a excess of high redshift galaxies, being it greater for models with a lower value of η : the model with

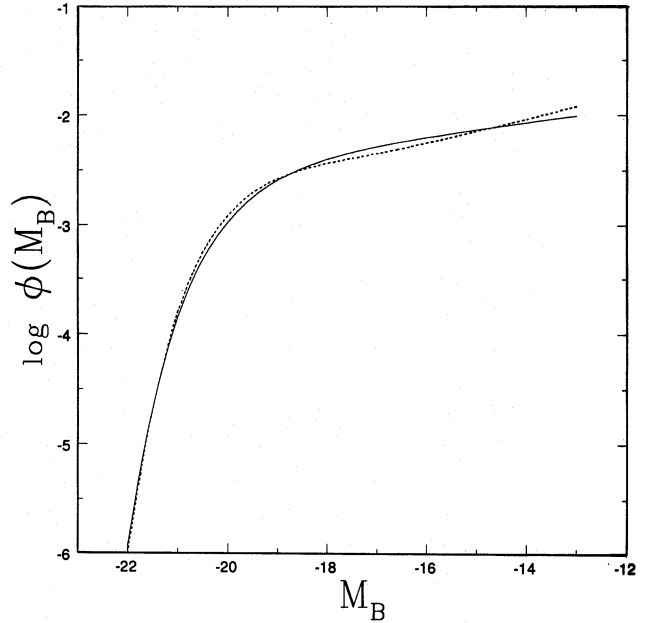


Fig. 4. The logarithm of the LFG is plotted here (dotted line) along with its Schechter fit (solid line). The values for the parameters α , ϕ^* , and M^* are given in the text.

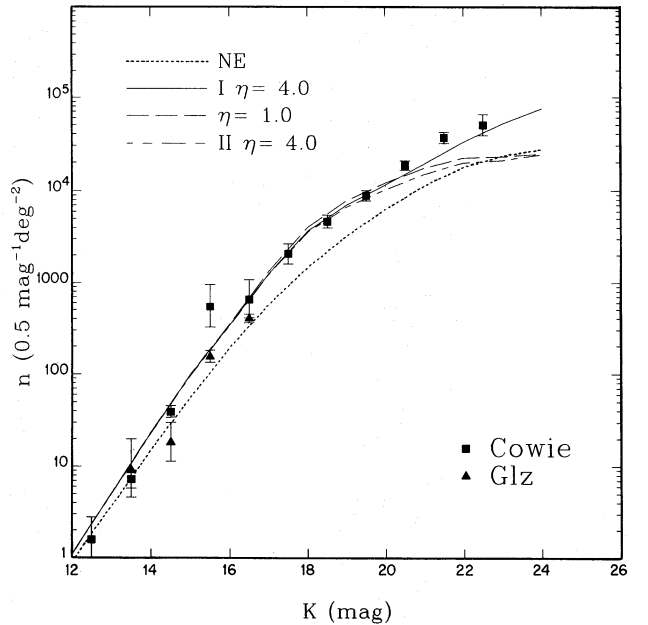


Fig. 5. Number of galaxies against K magnitude for the same models as Figure 3, except that the NE KGB model has been replaced by one whose contribution to L^* in the K band due to starbursts is neglected (II $\eta = 4.0$).

$\eta = 1.0$ predicts that 27% of the galaxies have $z > 0.7$ in the $21.0 \leq b_J \leq 22.5$ range, clearly inconsistent with the 5% derived by Colless et al. This is interesting since it could be a manner to discriminate

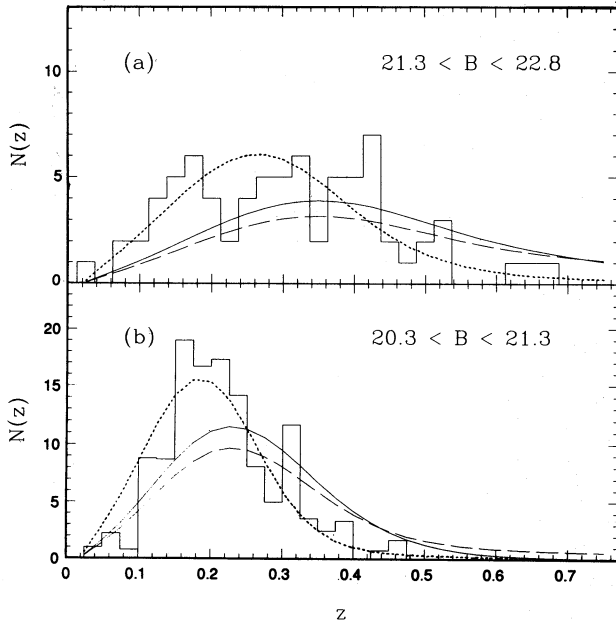


Fig. 6. Redshift distributions in two intervals of B magnitude: (a) $20.0 \leq b_J \leq 21.0$, and (b) $21.0 \leq b_J \leq 22.5$. Data are from Broadhurst et al. (1988) and Colless et al. (1990, 1993). The approximate color relationships $B = b_J + 0.18$ and $B = b_J + 0.16(b_J - r_F)$ for Broadhurst et al. and Colless et al. data, has been used, respectively. The two merger-driven and our NE models are plotted. The line code is the same as in Figure 3.

between models with number luminosity from those with luminosity evolution. The model with $\eta = 4.0$ predicts that about 13% of galaxies have $z > 0.7$, not too different from the observed 5%.

It appears difficult to reduce the number of high redshift galaxies by changing the parameters of the LF of interacting galaxies, subject to the constraints that: (1) a small fraction ($< 5\%$) of galaxies are strongly interacting at the present time, (2) the slope at the faint end is that of the total luminosity function, and (3) the characteristic luminosity of this population, L_I^* , is greater than the one of E/SO galaxies. For the sake of the argument, let us assume we increase further the value of the parameter η . One might think this would give us a better fit, but the point is that the fraction of galaxies greater than 0.7 does not decrease much by increasing the value of η ; for example, for $\eta = 10$ it is just 12% compared to the 13% for $\eta = 4$! This point can be explained as follows: as the η value increases the L_I^* decreases as

$$M_I^* = M_I^*(0) - 2.5(3 - \eta)\log(1 + z) ,$$

so the number of high- z galaxies decreases (improving the fit) but at the same time the number of moderate z galaxies increases due to the $(1 + z)^\eta$ law

(worsening the fit). At the end, the decrease of the fraction of galaxies with $z > 0.7$ is very small. We took the value of $\eta = 4$ as a reasonable estimate of the amount of mergers at $z = 0.4$ and as an acceptable fit to the z -distribution.

4. CONCLUSIONS

Differences of up to 0.25 mag in $V - K$ are found when various photometric calibrations are used. On the other hand, a smaller difference, 0.1 mag in $V - K$, is found when we compare the results that come from using two reasonable IMFs, the so-called KTG IMF and the Salpeter one. This is certainly negligible as far as the B or K number distributions calculations are concerned.

By using the best parameters we have in the literature for the LFs of the different classes of galaxies and for the mix of them, we arrive to the conclusion that number and luminosity evolution of the galaxy luminosity function are important ingredients in the explanation of the excess observed in the B -counts. Our merger-driven models require little evolution both in number and luminosity; for example, at $z = 0.4$ the total number of galaxies has just increased by 14% and the fraction of I galaxies is just 17% (model with $\eta = 4.0$). Moreover, luminosity evolution is such that a model with $\eta = 4.0$ predicts that about 13% of galaxies have $z > 0.7$ in the $21.0 < m_b < 22.5$ range. Models with more emphasis in number evolution reproduce better the redshift distributions (the $\eta = 4.0$ model as compared with the $\eta = 1.0$ one), as it should be expected. Despite the relative success of our models, the excess of high- z galaxies predicted by them indicates us that number and luminosity evolution may not be the whole story.

I would like to thank M. Peimbert and D. Dultzin for their careful reading of the manuscript. I am grateful to the anonymous referee for his/her comments on the manuscript. This paper was supported in part by DGPA, UNAM, through grant IN-1000994.

REFERENCES

- Babul A., & Rees, M.J. 1992, MNRAS, 255, 346
- Bessell, M.S., & Brett, J.M. 1988, PASP, 100, 1134
- Broadhurst, T.J., Ellis, R.S., & Shanks, T. 1988, MNRAS, 235, 827
- Broadhurst, T.J., Ellis, R.S., & Glazebrook, K. 1992, Nature, 355, 55
- Bruzual, A.G. 1983, ApJ, 273, 105
- . 1992, in Cosmology and Large-Scale Structure in the Universe, ed. R.R. de Carvalho (ASP, 24), 43
- Bruzual, A.G., & Charlot, S. 1993, ApJ, 405, 538
- Carlberg, R.G., & Charlot, S. 1992, ApJ, 397, 5
- Charlot, S., & Bruzual, A.G. 1991, ApJ, 367, 126
- Cole, S., Ellis, R.S., Broadhurst, T.J., & Colless, M.M. 1994, MNRAS, 267, 541

- Colín, P., Schramm, D.N., & Peimbert, M. 1994, *ApJ*, 426, 459 (CSP)
- Coleman, G.D., Wu, C.-C., & Weedman, D.W. 1980, *ApJS*, 43, 393 (CWW)
- Colless, M.M., Ellis, R.S., Taylor, K., & Hook, R.N. 1990, *MNRAS*, 244, 408
- Colless, M.M., Ellis, R.S., Broadhurst, T.J., Taylor, K., & Peterson, B.A. 1993, *MNRAS*, 261, 19
- Colless, M., Schade, D., Broadhurst, T.J., & Ellis, R.S. 1994, *MNRAS*, 267, 1108
- Cowie, L.L., Songaila, A., & Hu, E.M. 1991, *Nature*, 354, 460
- Cowie, L.L., Gardner, J.P., Wainscoat, R.J., & Hodapp, K.W. 1994, *ApJ*, 434, 114
- de Lapparent, V., Geller, M.J., & Huchra, J.P. 1989, *ApJ*, 343, 1
- Eales, S. 1993, *ApJ*, 404, 51
- Efstathiou, G., Ellis, R.S., & Peterson, B.A. 1988, *MNRAS*, 232, 431
- Efstathiou, G., Bernstein, G., Katz, N., Tyson, J.A., & Guhathakurta, P. 1991, *ApJ*, 380, L47
- Ferguson, H.C., & Sandage, A. 1991, *AJ*, 101, 765
- Fukugita, M., Takahara, F., Yamashita, K., & Yoshii, Y. 1990, *ApJ*, 361, L1
- Gardner, J.P., Cowie, L.L., & Wainscoat, R.J. 1993, *ApJ*, L9
- Griffiths, R.E. et al. 1994a, *ApJ*, 437, 67
- Griffiths, R.E. et al. 1994b, *ApJ*, 435, L19
- Guiderdoni, B., & Rocca-Volmerange, B. 1987, *A&A*, 186, 1
- Infante, L., & Pritchett, C.J. 1994, preprint
- Johnson, H. L. 1966, *ARA&A*, 4, 193
- Kroupa, P., Tout, C.A., & Gilmore, G. 1993, *MNRAS*, 262, 545
- Koo, D.C., Gronwall, C., & Bruzual, G.A. 1993, *ApJ*, 415, L21 (KGB)
- Lilly, S.J., Cowie, L.L., & Gardner, J.P. 1991, *ApJ*, 369, 79
- Lonsdale, C.J., & Chokshi, A. 1993, *AJ*, 105, 1333
- Loveday, J., Peterson, B.A., Efstathiou, G., & Maddox, S.J. 1992, *ApJ*, 390, 338
- Maddox, S.J., Sutherland, W.J., Efstathiou, G., Loveday, J., & Peterson, B.A. 1990, *MNRAS*, 247, 1P
- McGaugh, S.S. 1994, *Nature*, 367, 538
- Metcalfe, N., Shanks, T., Fong, R., & Jones, L.R. 1991, *MNRAS*, 249, 498
- Peimbert, M., Sarmiento, A., & Colín, P. 1994, *RevMexAA*, 28, 181
- Pence, W. 1976, *ApJ*, 203, 39
- Pilyugin, L.S. 1993, *A&A*, 94, 175
- Sandage, A., Binggeli, B., & Tammann, G.A. 1985, *AJ*, 90, 1759
- Schaller, G., Schaerer, D., Meynet, G., & Maeder, A. 1992, *A&AS*, 96, 269
- Schmidt-Kaler, T.H. 1982, in *Landolt-Bornstein New Series*, Vol. 2b, *A&A, Stars and Star Clusters*, ed. K. Schaifers & H.H. Voigt (New York: Springer-Verlag)
- Soifer, B.T. et al. 1994, *ApJ*, 420, L1
- Tyson, J.A. 1988, *AJ*, 96, 1
- Worthey, G. 1994, *ApJS*, 95, 107
- Yoshii, Y. 1993, *ApJ*, 403, 552
- Yoshii, Y., & Takahara, F. 1988, *ApJ*, 326, 1
- Zucca, E., Pozzetti, L., & Zamorani, G. 1994, *MNRAS*, in press

Pedro Colín: University of Toronto, Dept. of Astronomy, 60 St. George Street, Toronto, Ontario M5S 1A1, Canada. (colin@moonray.astro.utoronto.ca).

